Association of Corneal Hysteresis With Lamina Cribrosa Curvature in Primary Open Angle Glaucoma

Kyoung Min Lee,[1,2] Tae-Woo Kim,[1,3] Eun Ji Lee,[1,3] Michaël J. A. Girard,[4,5] Jean Martial Mari,[6] and Robert N. Weinreb[7]

[1]Department of Ophthalmology, Seoul National University College of Medicine, Seoul, Korea
[2]Department of Ophthalmology, Seoul National University Boramae Medical Center, Seoul, Korea
[3]Department of Ophthalmology, Seoul National University Bundang Hospital, Seongnam, Korea
[4]Department of Bioengineering, National University of Singapore, Singapore
[5]Singapore Eye Research Institute, Singapore
[6]Université de la Polynésie française, Tahiti, French Polynesia
[7]Hamilton Glaucoma Center, Shiley Eye Institute, and Viterbi Family Department of Ophthalmology, University of California, San Diego, California, United States

Correspondence: Tae-Woo Kim, Department of Ophthalmology, Seoul National University Bundang Hospital, Seoul National University College of Medicine, 82, Gumi-ro, 173 Beongil, Bundang-gu, Seongnam, Gyeonggi-do 463-707, Korea; twkim7@snu.ac.kr.

Submitted: March 13, 2019
Accepted: September 8, 2019

Citation: Lee KM, Kim T-W, Lee EJ, Girard MJA, Mari JM, Weinreb RN. Association of corneal hysteresis with lamina cribrosa curvature in primary open angle glaucoma. *Invest Ophthalmol Vis Sci*. 2019;60:4171–4177. https://doi.org/10.1167/iovs.19-27087

Purpose. To investigate whether corneal biomechanical properties are associated with the lamina cribrosa (LC) curvature in eyes with primary open angle glaucoma (POAG).

Methods. Corneal biomechanical properties and LC curvature were assessed in 65 treatment-naïve POAG patients. Corneal biomechanical properties, including corneal hysteresis (CH), corneal resistance factor (CRF), and corneal-compensated intraocular pressure (IOPcc), were measured using an ocular response analyzer (ORA; Reichert Ophthalmic Instruments). LC curvature was assessed by measuring the LC curvature index (LCCI) on B-scan images obtained using spectral-domain optical coherence tomography (OCT). The LCCI was determined by measuring LC curve depth on the anterior LC surface and the width of the reference line.

Results. The LCCI was correlated with CH ($P = 0.001$), CRF ($P = 0.012$) and IOPcc ($P = 0.001$) in the univariate analysis. To adjust multicollinearity, principal component analysis was performed, and multivariate regression analyses were conducted using one variable from each component. The larger LCCI was associated with larger IOPcc ($P < 0.001$), smaller CRF ($P = 0.001$) and smaller CH ($P < 0.001$).

Conclusions. Lower CH was associated with a more posteriorly curved LC in treatment naïve POAG patients. This finding may provide a basic explanation for the reported association between CH and an increased risk for glaucoma development and progression, and support a potential value of CH for risk assessment for glaucoma.

Keywords: Corneal hysteresis, ocular response analyzer, lamina cribrosa, spectral-domain optical coherence tomography

Intraocular pressure (IOP) plays a pivotal role in glaucomatous optic nerve damage,[1] and the lamina cribrosa (LC) is a key structure for understanding IOP-related mechanical damage of the optic nerve.[2,3] An experimental study demonstrated that the LC deforms posteriorly upon IOP elevation prior to detectable retinal nerve fiber layer (RNFL) loss.[4] Because optic nerve axons pass through laminar pores, LC deformation may induce stress and insult to the axons. This stress, in turn, may initiate or accelerate retinal ganglion cell apoptosis through various mechanisms, including blockade of axoplasmic flow.[5]

Studies have shown that LC position and curvature change in accordance with changes in IOP. Reduction in IOP, either through surgery[6–8] or medication,[9] was shown to result in anterior shift of the LC position and flattening of the LC curve. In addition, re-elevation of IOP, due to a decrease in bleb function, in patients who underwent trabeculectomy resulted in the posterior movement of anteriorly-shifted LC.[8,10] These findings suggest that IOP-related stress is a key driving force that induces and maintains posterior LC bowing. However, the degree of posterior LC deformation is not simply dependent on IOP level but is influenced by other factors, including the material properties of the LC.[11]

Because both sclera and cornea have a similar collagen content,[12] their material properties may be related. It would, therefore, be of interest to determine whether corneal properties, such as corneal hysteresis (CH), are associated with the configuration of LC, which also has a collagenous part.[13] The purpose of the study was to determine whether CH is associated with posterior bowing of the LC, as assessed by the LC curvature index (LCCI), in eyes with treatment-naïve primary open angle glaucoma (POAG).

Methods

Participants

This investigation was based on the database of POAG patients included in the Investigating Glaucoma Progression Study

(IGPS), which is an ongoing prospective study at the Seoul National University Bundang Hospital Glaucoma Clinic. Written informed consent was obtained from all subjects, and the study protocol was approved by the Institutional Review Board of Seoul National University Bundang Hospital and followed the tenets of the Declaration of Helsinki.

Subjects who were enrolled in the IGPS underwent a comprehensive ophthalmic examination, including visual acuity assessment, Goldmann applanation tonometry, refraction tests, slit-lamp biomicroscopy, gonioscopy, and dilated stereoscopic examination of the optic disc. All subjects also underwent disc photography and red-free fundus photography (EOS D60 digital camera; Canon, Utsunomiyashi, Tochigiken, Japan), circumpapillary RNFL scanning and enhanced depth imaging (EDI) of the optic nerve head by spectral-domain optical coherence tomography (SD-OCT, Spectralis; Heidelberg Engineering, Heidelberg, Germany), and standard automated perimetry (Humphrey Field Analyzer II 750; 24–2 Swedish interactive threshold algorithm; Carl Zeiss Meditec, Dublin, CA, USA). In addition, all subjects underwent measurements of corneal curvature (KR-1800; Topcon, Tokyo, Japan), central corneal thickness (CCT, Orbscan II; Bausch & Lomb Surgical, Rochester, NY, USA), and axial length (IOL Master version 5; Carl Zeiss Meditec). Although initial enrollment in the IGPS began in 2011, additional tests have been added as new instruments have become available. Since September 2014, CH has been measured in the treatment-naïve POAG patients using the Ocular Response Analyzer (ORA v. 2.02; Reichert Ophthalmic Instruments, Depew, NY, USA).

The IGPS excluded subjects with a best-corrected visual acuity of <20/40, a history of intraocular surgery other than cataract extraction and glaucoma surgery, or any intraocular disease (e.g., diabetic retinopathy or retinal vein occlusion) or neurologic disease (e.g., pituitary tumor) that could cause visual field loss.

Patients included in the present study were required to be newly diagnosed with POAG. POAG was defined as the presence of glaucomatous optic nerve damage and associated visual field defect without ocular disease or conditions that might elevate IOP, and an open angle on gonioscopy. A glaucomatous visual field change was defined as (1) outside normal limit on glaucoma hemifield test, (2) three abnormal points with a <5% probability of being normal, including 1 with a probability <1% by pattern deviation, or (3) a pattern standard deviation of 5% if the visual field was otherwise normal, as confirmed on two consecutive tests. Visual field measurements were considered reliable when the rate of false-positive/negative results was <25% and the rate of fixation losses was <20%.

Eyes that had undergone corneal refractive surgery, coexisting corneal dystrophy that could affect CH, or those with optic disc torsion >15° or a tilt ratio (minimum-to-maximum optic disc diameter) <0.75 were excluded.[14,15] Eyes were also excluded when good-quality images (i.e., quality score >15) could not be obtained at more than five sections of EDI SD-OCT disc scans (if the quality score did not reach 15, the image-acquisition process automatically stopped and the image of that section was not obtained), or when the images did not allow clear delineation of the anterior LC border at the measurement points on more than two selected B-scans. If both eyes were eligible, one was randomly chosen for analysis.

Measurement of Corneal Biomechanical Properties

Corneal material properties were measured by the ORA. To minimize the effects of topical anesthetics, measurements in all eyes were performed at least 10 minutes before Goldmann applanation tonometry. As the software generates a waveform score of 0 to 10, with higher values representing more accurate measurements, only readings with waveform scores ≥7 were included in the data analysis. At least two measurements were obtained per eye, with the highest waveform scores used for the analysis.

Details of the operation of the ORA have been described previously.[16] Briefly, the ORA emits collimated air pulses, converting convex to concave corneas, with these corneas recovering their original convexity within milliseconds. During this process, corneal flattening is observed at two pressure levels: from convex to concave (P_1) and from concave to convex (P_2). The difference between these pressure levels ($P_1 - P_2$) was defined as the CH, a measure of the energy dissipated by the material properties of the cornea during the stress-strain cycle.[17]

The ORA also measures several other parameters. The corneal resistance factor (CRF) was calculated as $P_1 - k \times P_2$, with k derived from empirical evaluation of P_1, P_2, and CCT. This modified parameter was found to be more strongly associated with CCT than with CH and it is relatively unaffected by IOP.[17] CRF is thought to reflect overall resistance against stresses that are relatively unaffected by changes in IOP, whereas CH is affected by both IOP and tissue resistance. The ORA also provides an estimate of IOP that is less influenced by corneal properties than that provided by Goldmann applanation tonometry, with this ORA-estimated IOP called corneal-compensated IOP (IOPcc).[18,19] IOPcc is regarded as being better able to predict clinically relevant outcomes than conventional IOP measurement.[20]

Enhanced Depth Imaging SD-OCT of the Optic Disc

The optic nerve head (ONH) of each eye was imaged by OCT (Heidelberg Engineering) using the EDI technique. The details and advantages of this technology for evaluating the LC have been described previously.[21,22] Imaging was performed using a 10° × 15° rectangle covering the optic disc. Scanning of this rectangle consisted of approximately 70 sections, located 30 to 34 μm apart, with the slicing distance determined automatically by the machine. The average number of frames per section was 42, which provided the best tradeoff between image quality and patient cooperation.[22] Corneal curvature was entered into the OCT system (Heidelberg Engineering) prior to scanning, thus removing any magnification error. To enhance the visibility of the peripheral LC, all images were post-processed using adaptive compensation.[23,24]

Quantification of the LC Curvature

LC curvature was quantified using the LC curvature index (LCCI), which was defined as the inflection of a curve representing a section of the LC.[25–27] The LCCI of each eye was measured on horizontal B-scan images at seven locations equidistant across the vertical optic disc diameter. The measurements obtained from these seven B-scans were used to calculate the mean LCCI of the eye. To enhance the visibility of the peripheral LC, all images were post-processed using adaptive compensation,[23,24] and measurements were determined using ImageJ software (version 1.51, http://imagej.nih.gov/ij/; provided in the public domain by the National Institutes of Health, Bethesda, MD, USA) by two glaucoma specialists (KML, EJL) who were blinded to patients' clinical information.

To measure the LCCI, a reference line was drawn on each B-scan by connecting the two points on the anterior LC surface that met the lines drawn from each termination point at Bruch's membrane (BM), perpendicular to the reference line

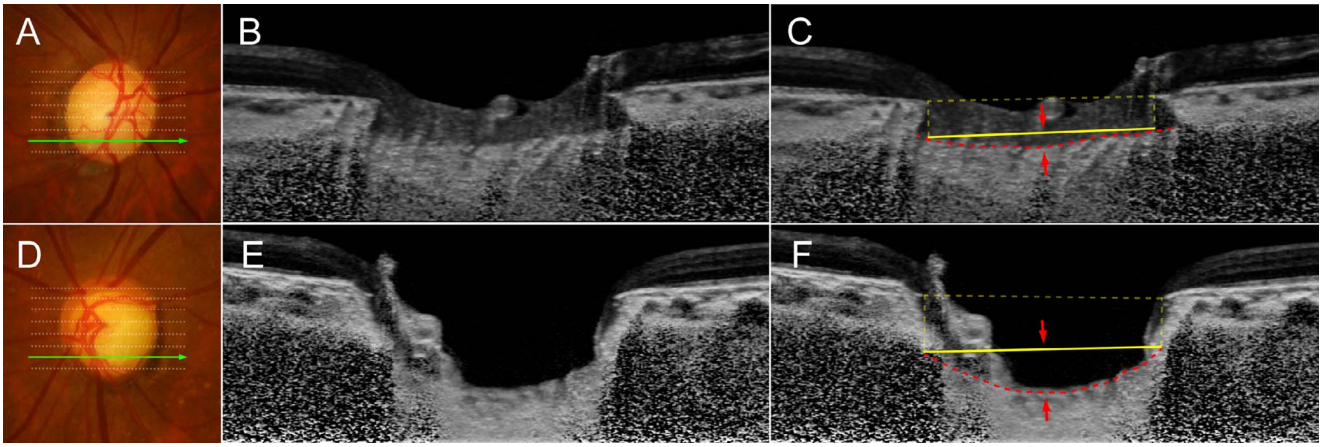

Figure 1. LCCI in eyes without (**A**–**C**) and with (**D**–**F**) the posterior bowing of the LC. (**A**, **D**) Disc photographs showing seven *horizontal* lines that indicate the locations at which the measurements were performed. *Green arrows* indicate where B-scan OCT images of (**B**) and (**E**) were obtained. (**B**, **E**) B-scan OCT images after adaptive compensation. (**D**, **F**) Same images with the lines demarcated along the anterior surface of LC (*red dashed lines*). Reference lines (*yellow lines*) were defined by the projection of Bruch's membrane opening (*yellow dashed lines*). LC curvature depth was defined the lineal distance to the maximally depressed point from the reference line (between the *red arrows*). LCCI was calculated by dividing LCCD by the width of the reference line (*W*) and multiplying by 100.

for the BM opening. The length of this reference line was defined as the width (W), the maximum depth from this reference line to the anterior LC surface was defined as the LC curve depth (LCCD; Fig. 1), and the LCCI of each eye was calculated as (LCCD/W) × 100. Because the curvature was normalized to the LC width, it describes the shape of the LC independent of the actual size of the ONH. Similar normalization was also used in the measurement of iris curvature.[25] Only the LC within the BM opening was considered, because the LC was often not clearly visible outside this opening. In eyes with LC defects, the LCCD was measured using a presumed anterior LC surface that best fit the curvature of the remaining part of the LC or excluding the area of LC defect.

To evaluate the interobserver reproducibility of this method, 20 randomly selected SD-OCT datasets were evaluated by two independent examiners (KML, EJL), who calculated the intraclass correlation coefficient (ICC) and limit of agreement using Bland-Altman analysis.

Data Analysis

Linear regression analysis and Pearson's correlation analysis were used to evaluate the associations between the LCCI and ORA parameters. Due to the multicollinearity of ORA parameters, principal component analysis was utilized to reduce the number of dimensions. The threshold for statistical significance was set at $P < 0.05$. All statistical analyses were performed with commercially available software (Stata version 14.0; StataCorp, College Station, TX, USA) and R statistical package version 3.4.3 (available at http://www.r-project.org; assessed December 5, 2017). Except where indicated otherwise, all data are presented as mean ± standard deviation (SD).

Table 1. Patient Clinical Demographics

	Study Population (n = 65)
Age, y	52.7 ± 14.1
Male/female	26/39
Spherical equivalent, D	−2.15 ± 2.96
Central corneal thickness, μm	550.5 ± 40.9
Axial length, mm	24.55 ± 1.63
IOP, mm Hg	14.4 ± 3.2
IOPcc, mm Hg	15.5 ± 3.6
CH, mm Hg	10.8 ± 2.3
CRF, mm Hg	10.7 ± 2.7
LCCI	9.5 ± 2.0
RNFL thickness, μm	76.4 ± 14.8
Mean deviation, dB	−5.05 ± 5.92

D, diopters; dB, decibel.

Results

The study initially enrolled 87 eyes of 87 treatment-naïve POAG patients. Of these, 22 eyes were excluded, 10 because they had undergone prior corneal refractive surgery, 9 because their optic discs were tilted, 2 because B-scan image quality was poor, and 1 because of coexisting corneal dystrophy. Thus, 65 eyes of 65 subjects were evaluated; their demographic and clinical characteristics are summarized in Table 1.

The LCCI measurement showed excellent intraobserver (ICC = 0.985 [95% confidence interval: 0.942–0.995], two-way mixed-effects model, absolute agreement) and interobserver (ICC = 0.975 [95% confidence interval: 0.939–0.990], two-way random effects model, absolute agreement) reproducibility. The intraobserver and interobserver limits of agreement for measurements of the LCCI were −0.3 (lower, 95% confidence interval: −0.5 to −0.1) and 0.6 (upper, 95% confidence interval: 0.4 to 0.8), and −0.8 (lower, 95% confidence interval: −1.1 to −0.5) and 0.7 (upper, 95% confidence interval: 0.4 to 1.0), respectively (Supplementary Fig. S1).

CH was correlated with IOPcc ($r = -0.300$, $P = 0.015$), CRF ($r = 0.899$, $P < 0.001$), and CCT ($r = 0.531$, $P < 0.001$). CRF was correlated with CCT ($r = 0.605$, $P < 0.001$). IOPcc was not correlated with CRF ($r = 0.148$, $P = 0.240$) or CCT ($r = 0.111$, $P = 0.378$; Fig. 2A). Principal component analysis was used to identify basic components from ORA parameters and CCT. The two principal components (PCs) explained 88% of the total variance in the data (59%, PC_1; 29%, PC_2; Fig. 2B). Among them, IOPcc was exclusively dependent on PC_2, CRF and CCT were exclusively dependent on PC_1, whereas CH was dependent on both PC_1 and PC_2 (Fig. 2B).

Linear regression analysis was performed based on this reduction of dimension. Univariate analysis showed that higher LCCI was significantly associated with higher IOPcc ($P = 0.001$), lower CRF ($P = 0.012$), and lower CH ($P < 0.001$; Table

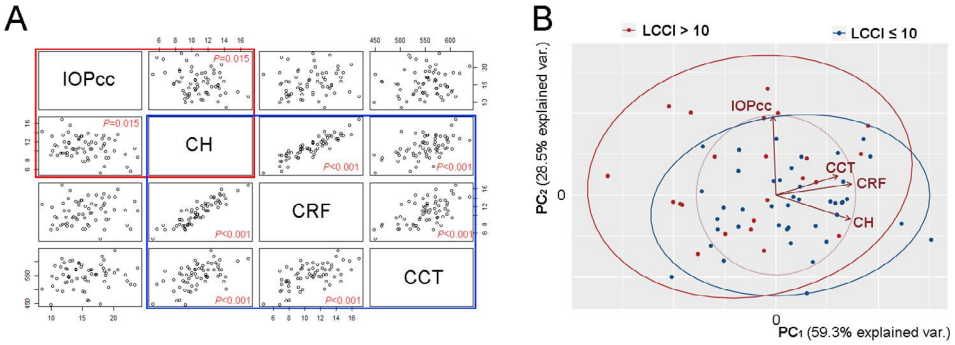

Figure 2. **(A)** A scatter plot matrix showing correlations between parameters of the ORA. Based on their correlations, two clusters are identified: One cluster (*red box*) consists of IOPcc and corneal hysteresis CH. The other cluster (*blue box*) consists of CH, CRF, and CCT. CH is belonging to both clusters. **(B)** Principal component analysis of ORA parameters. A biplot shows that principal component 1 (PC_1) and principal component 2 (PC_2) explains 59.3% and 28.5% of total variance of ORA parameters, respectively. The relation of each ORA parameter to both components is drawn as an arrow. A parallel arrow means that this parameter is entirely dependent on that component, while a perpendicular arrow means complete irrelevance between them. IOPcc is directly related to PC_2 (*y-axis direction*), while CRF and CCT are related to PC_1 (*x-axis direction*). Please note that CH is not perpendicular to both components, which indicates that it is related both components. The LCCI of each subject is drawn in the biplot. Arbitrarily, the more steeply (LCCI >10) and the less steeply curved LC (LCCI ≤10) are distinguished using different colors. Each ellipse indicates the 95% probability area of each group. Despite many overlaps, the more curved LC tends to locate on the left side along PC_1 and on the up side along PC_2. This indicates that more curved LC is associated with smaller PC_1, which is correlated with smaller CH, CRF, and CCT (resistance component), and larger PC_2 which is correlated with IOPcc (pressure component).

2, Fig. 3). Lower CCT was correlated with LCCI with marginal significance ($P = 0.054$; Table 2). Because these parameters showed multicollinearity, multivariate analysis was performed, using one variable that reflected each component identified by principal component analysis: (1) CRF–PC_1 and IOPcc–PC_2, (2) CCT–PC_1 and IOPcc–PC_2, and (3) CH, as this parameter reflected both PC_1 and PC_2. In model 1, LCCI was significantly associated with IOPcc ($P < 0.001$) and CRF ($P = 0.001$). In model 2, LCCI was significantly associated with IOPcc ($P < 0.001$) and CCT ($P = 0.012$). In model 3, LCCI was significantly associated with CH ($P < 0.001$). Adjusted R^2 was highest in model 1, although a similar value was obtained using only one variable (i.e., CH) in model 3 (Table 2).

Discussion

In this study, we investigated whether the degree of LC deformation was associated with CH in treatment-naïve POAG patients. We found that patients with lower CH had more curved LC. In addition, the LCCI was positively correlated with IOPcc and inversely correlated with CRF. This study was novel in its assessment of LC curves and corneal biomechanical properties in treatment-naïve POAG patients.

LCCI was used to measure the degree of LC curvature. The validity of LCCI for evaluating LC morphology is supported by several studies. The change of LC morphology after IOP lowering surgery was well characterized using LCCI.[26] In addition, LCCI was excellent in differentiating between glaucomatous and healthy eyes,[27] and was able to predict the rate of future RNFL thinning in glaucoma suspects.[28] More recently, a correspondence between larger regional LCCI and location of RNFL defects was reported in POAG eyes with hemifield defects.[29] These results indicate that LCCI is a valid parameter to evaluate IOP-related glaucomatous LC strain or morphology.

Experimentally, posterior bowing of the LC has been demonstrated after IOP elevation.[3,30,31] Conversely, reduction of LC curvature occurred after IOP lowering treatment in glaucoma patients.[6,9,26,32] Moreover, interindividual variation of LCCI of healthy subjects were confined within a certain range (95th percentile was 9.51).[33] These findings suggest that the innate LC is slightly curved and elastic, thereby being posteriorly bowed when IOP increases and becoming less curved when IOP decreases. Therefore, although the possibility of an inborn large curvature cannot be ruled out completely, an eye with a relatively large LCCI is more likely to have experienced a certain degree of posterior LC deformation.

Ideal elastic tissue will return to its original configuration once the external stress has been removed. However, connective tissues, such as cornea and LC, have elements of both elasticity and viscosity, with some energy being dissipated when a stress is applied. This loss of dissipated energy during the stress-strain cycle is defined as hysteresis.[17] The degree of hysteresis is determined by both the applied pressure and the material properties that dissipate stress in response to elastic changes. Similarly, IOP-induced stress applied to the LC would

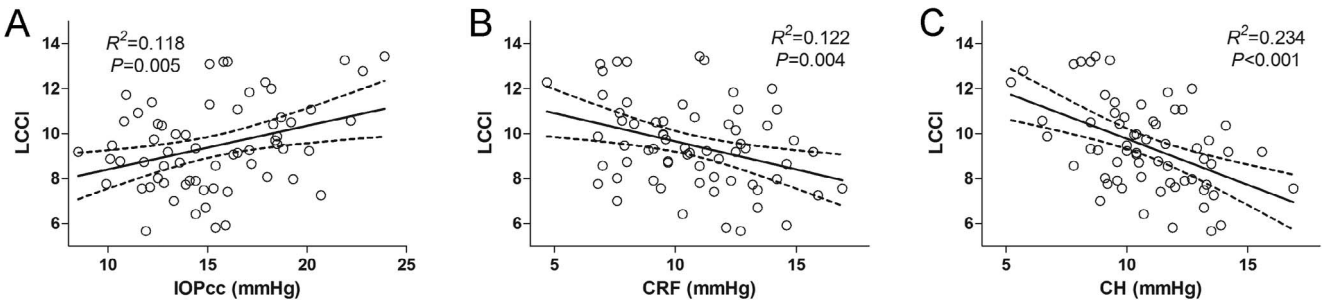

Figure 3. Association between the LCCI and ORA parameters including **(A)** IOPcc, **(B)** CRF, and **(C)** CH.

Investigative Ophthalmology & Visual Science

TABLE 2. Factors Associated With More Posteriorly Curved LC at Initial Visit

	Univariate Analysis			Multivariate Analysis (Model 1)*			Multivariate Analysis (Model 2)*			Multivariate Analysis (Model 3)*		
	Coefficient	95% CI	*P*	Coefficient	95% CI	*P*	Coefficient	95% CI	*P*	Coefficient	95% CI	*P*
Age, years	0.004	(−0.032 to 0.040)	0.827									
Female sex	0.393	(−0.628 to 1.414)	0.444									
Axial length, mm	0.007	(−0.304 to 0.317)	0.966									
IOP, mm Hg	0.071	(−0.088 to 0.230)	0.377									
IOPcc, mm Hg	**0.219**	**(0.089 to 0.349)**	**0.001**	**0.251**	**(0.129 to 0.372)**	**<0.001**	**0.237**	**(0.112 to 0.363)**	**<0.001**			
CH, mm Hg	**−0.411**	**(−0.605 to 0.217)**	**<0.001**							**−0.411**	**(−0.605 to 0.217)**	**<0.001**
CRF, mm Hg	**−0.230**	**(−0.408 to −0.052)**	**0.012**	**−0.279**	**(−0.440 to −0.118)**	**0.001**						
CCT, µm	−0.012	(−0.024 to 0.000)	0.054				**-0.014**	**(−0.025 to −0.003)**	**0.012**			
RNFL thickness, µm	−0.018	(−0.051 to 0.016)	0.305									
Mean deviation, dB	−0.025	(−0.110 to 0.060)	0.559									
R^2				0.291			0.235			0.221		
Adjusted R^2				0.268			0.210			0.208		

* Variables with $P < 0.10$ in the univariate analysis were included in the multivariate analysis. Because of multicollinearity between IOPcc, CH, CRF, and CCT, three models were constructed. Significant values ($P < 0.05$) are shown in bold.

partly dissipate. When the dissipation is large, only a small fraction of energy would be involved in LC deformation. Therefore, LC hysteresis may play a significant role in the posterior bowing of the LC.

The association between LC and corneal hysteresis could be understood in two ways. First, cornea and sclera have a similar collagen content,[12] and LC is also rich of collagen.[13] It is possible that the collagen in LC may have similar material property with that in the corneal and scleral collagen within an individual. The embryologic origins of them, however, are complicated,[34] and the relationship of their material properties are not certain yet. Alternatively, it may also be hypothesized that association between LC and corneal hysteresis have been acquired after birth at least in part. Internal pressure within the globe would affect both ends of the scleral canal (i.e., LC and cornea). In this situation, LC and corneal hysteresis are both affected by the same pressure, true IOP, thereby they might be correlated.

Energy dissipation may also be relevant not only with the static IOP level but also with dynamic IOP changes induced by ocular perfusion, blinking, etc. However, Agoumi et al.[35] demonstrated that anterior LC surface was noncompliant to acute IOP elevation induced by ophthalmodynamometry. Therefore, it is likely that the degree of energy dissipation during dynamic IOP change may not be a predominant factor for determining the LC morphology. Nonetheless, cumulative effect of energy dissipation upon instant IOP change over long time may have some influence on the LC morphology.

Univariate analysis showed that CCT was not associated with LCCI. CCT was only associated with LCCI when considered together with IOPcc in the multivariate analysis (model 2). At a given level of measured IOP, variation in CCT can reflect variation in "true IOP." This finding suggests that LCCI is influenced by true IOP. In addition, statistical significance ($P = 0.012$) of CCT in the multivariate analysis was less than that of CH ($P < 0.001$). This finding signifies that CH could be more practical parameter than CCT via reflecting both material properties (e.g., CCT and corneal stiffness) and internal globe pressure (true IOP).[36] This does not necessarily mean that lower CH is a causal factor to induce greater posterior LC deformation. It is possible that eyes with lower CH may have higher true IOP. Currently, CCT is measured routinely in clinical practice as a measure to correct the IOP and as a potential factor related with glaucoma progression.[37–39] Further study may be needed to evaluate whether CH may have additional clinical value over CCT in predicting the development and progression of glaucoma.

CH has been shown to predict glaucoma development[40] and progression.[41–45] The association between CH and LCCI provides a plausible explanation for the association of CH with glaucoma progression.[41–45] In eyes with smaller hysteresis, pressure would not be dissipated too much. Thus, a higher proportion of IOP-derived energy would be used in elastic changes resulting in greater LC deformation (Fig. 4). This, in turn, would likely promote axonal damage through diverse mechanisms.[3]

The LCCI was not correlated with the disease severity parameters such as mean deviation of visual field test or average RNFL thickness. This is consistent with our previous study.[27] An experimental study demonstrated that LC bowing occurs earlier than RNFL loss.[4,35] This indicates that the RNFL loss occurs with time after the LC deformation. Therefore, the degree of RNFL loss is likely dependent both on the duration of LC deformation and the degree of LC deformation. In addition, glaucoma is a multifactorial disease in which non-IOP related factors (e.g., vascular factors) may also play a role in the optic nerve damage. Therefore, severe optic nerve damage may be

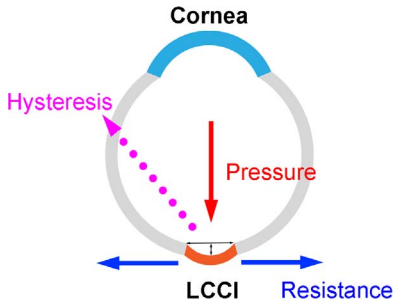

FIGURE 4. Schematic diagram suggesting two components affecting the LCCI. The posterior bowing of LC would be the product of given pressure and tissue resistance, which comprised two principal components (PC_2 and PC_1 in Fig. 2B, respectively). Hysteresis represents the energy dissipated by material property of connective tissue during the stress-strain cycle. Therefore, hysteresis is a parameter related both pressure and tissue resistance. Assuming that corneal hysteresis is associated with LC hysteresis, smaller CH may implicate that LC is more prone to deform when IOP-induced stress is applied.

found without a large degree of LC deformation if non-IOP related factors play a predominant role in a given patient.[46]

This study had several limitations. First, due to its cross-sectional design, the prognostic value of higher LCCI and lower CH could not be addressed. Second, the LCCI reflects the loading of the LC along the axial direction, while there might be another source of LC deformation including tensile stiffening associated with scleral canal expansion.[47,48] Third, we used linear regression model even though stress/strain curves of cornea and LC might be nonlinear. Fourth, because eyes with tilted discs and eyes previously treated for glaucoma with antiglaucoma medications and/or surgery were excluded, our results cannot be applied to such eyes. Finally, we could not determine whether CH and CRF represent true hysteresis or resistance of LC because no method is currently available to directly measure the material properties of the LC.

In conclusion, CH was correlated with LC curvature in treatment naïve POAG patients, suggesting that both IOP and material property of LC are involved in the posterior LC deformation. This finding may provide a basic explanation for the reported association of CH with an increased risk for glaucoma development and progression, and support a potential value of CH for risk assessment for glaucoma.

Acknowledgments

Disclosure: **K.M. Lee**, None; **T.-W. Kim**, Reichert Ophthalmic Instruments (F); **E.J. Lee**, None; **M.J.A. Girard**, None; **J.M. Mari**, None; **R.N. Weinreb**, None

References

1. Weinreb RN, Aung T, Medeiros FA. The pathophysiology and treatment of glaucoma: a review. *JAMA*. 2014;311:1901–1911.
2. Quigley HA, Addicks EM, Green WR, Maumenee AE. Optic nerve damage in human glaucoma. II. The site of injury and susceptibility to damage. *Arch Ophthalmol*. 1981;99:635–649.
3. Burgoyne CF, Downs JC, Bellezza AJ, Suh JK, Hart RT. The optic nerve head as a biomechanical structure: a new paradigm for understanding the role of IOP-related stress and strain in the pathophysiology of glaucomatous optic nerve head damage. *Prog Retin Eye Res*. 2005;24:39–73.
4. He L, Yang H, Gardiner SK, et al. Longitudinal detection of optic nerve head changes by spectral domain optical coherence tomography in early experimental glaucoma. *Invest Ophthalmol Vis Sci*. 2014;55:574–586.
5. Downs CJ, Roberts MD, Sigal IA. Glaucomatous cupping of the lamina cribrosa: a review of the evidence for active progressive remodeling as a mechanism. *Exp Eye Res*. 2011; 93:133–140.
6. Lee EJ, Kim TW, Weinreb RN. Reversal of lamina cribrosa displacement and thickness after trabeculectomy in glaucoma. *Ophthalmology*. 2012;119:1359–1366.
7. Barrancos C, Rebolleda G, Oblanca N, Cabarga C, Munoz-Negrete FJ. Changes in lamina cribrosa and prelaminar tissue after deep sclerectomy. *Eye (Lond)*. 2014;28:58–65.
8. Lee EJ, Kim TW. Lamina cribrosa reversal after trabeculectomy and the rate of progressive retinal nerve fiber layer thinning. *Ophthalmology*. 2015;122:2234–2242.
9. Lee EJ, Kim TW, Weinreb RN, Kim H. Reversal of lamina cribrosa displacement after intraocular pressure reduction in open-angle glaucoma. *Ophthalmology*. 2013;120:553–559.
10. Lee EJ, Kim TW, Weinreb RN. Variation of lamina cribrosa depth following trabeculectomy. *Invest Ophthalmol Vis Sci*. 2013;54:5392–5399.
11. Quigley HA. The contribution of the sclera and lamina cribrosa to the pathogenesis of glaucoma: diagnostic and treatment implications. In: Bagetta G, Nucci C, eds. *Progress in Brain Research*. Elsevier; 2015:59–86.
12. Meek KM, Fullwood NJ. Corneal and scleral collagens—a microscopist's perspective. *Micron*. 2001;32:261–272.
13. Elkington AR, Inman CBE, Steart PV, Weller RO. The structure of the lamina cribrosa of the human eye: An immunocytochemical and electron microscopical study. *Eye (Lond)*. 1990; 4:42–57.
14. Vongphanit J, Mitchell P, Wang JJ. Population prevalence of tilted optic disks and the relationship of this sign to refractive error. *Am J Ophthalmol*. 2002;133:679–685.
15. Samarawickrama C, Mitchell P, Tong L, et al. Myopia-related optic disc and retinal changes in adolescent children from Singapore. *Ophthalmology*. 2011;118:2050–2057.
16. Luce DA. Determining in vivo biomechanical properties of the cornea with an ocular response analyzer. *J Cataract Refract Surg*. 2005;31:156–162.
17. Kotecha A. What biomechanical properties of the cornea are relevant for the clinician? *Surv Ophthalmol*. 2007;52(suppl 2):S109–S114.
18. Kotecha A, Elsheikh A, Roberts CR, Zhu H, Garway-Heath DF. Corneal thickness- and age-related biomechanical properties of the cornea measured with the ocular response analyzer. *Invest Ophthalmol Vis Sci*. 2006;47:5337–5347.
19. Medeiros FA, Weinreb RN. Evaluation of the influence of corneal biomechanical properties on intraocular pressure measurements using the ocular response analyzer. *J Glaucoma*. 2006;15:364–370.
20. Susanna BN, Ogata NG, Daga FB, Susanna CN, Diniz-Filho A, Medeiros FA. Association between rates of visual field progression and intraocular pressure measurements obtained by different tonometers. *Ophthalmology*. 2019;126:49–54.
21. Spaide RF, Koizumi H, Pozzoni MC. Enhanced depth imaging spectral-domain optical coherence tomography. *Am J Ophthalmol*. 2008;146:496–500.
22. Lee EJ, Kim TW, Weinreb RN, Park KH, Kim SH, Kim DM. Visualization of the lamina cribrosa using enhanced depth imaging spectral-domain optical coherence tomography. *Am J Ophthalmol*. 2011;152:87–95.e81.
23. Girard MJ, Strouthidis NG, Ethier CR, Mari JM. Shadow removal and contrast enhancement in optical coherence tomography images of the human optic nerve head. *Invest Ophthalmol Vis Sci*. 2011;52:7738–7748.

24. Mari JM, Strouthidis NG, Park SC, Girard MJ. Enhancement of lamina cribrosa visibility in optical coherence tomography images using adaptive compensation. *Invest Ophthalmol Vis Sci*. 2013;54:2238–2247.
25. Amini R, Whitcomb JE, Prata TS, et al. Quantification of iris concavity. *J Ophthalmic Vis Res*. 2010;5:211–212.
26. Lee SH, Yu DA, Kim TW, Lee EJ, Girard MJ, Mari JM. Reduction of the lamina cribrosa curvature after trabeculectomy in glaucoma. *Invest Ophthalmol Vis Sci*. 2016;57:5006–5014.
27. Lee SH, Kim TW, Lee EJ, Girard MJ, Mari JM. Diagnostic power of lamina cribrosa depth and curvature in glaucoma. *Invest Ophthalmol Vis Sci*. 2017;58:755–762.
28. Kim JA, Kim TW, Weinreb RN, Lee EJ, Girard MJA, Mari JM. Lamina cribrosa morphology predicts progressive retinal nerve fiber layer loss in eyes with suspected glaucoma. *Sci Rep*. 2018;8:738.
29. Kim JA, Kim TW, Lee EJ, Girard MJA, Mari JM. Lamina cribrosa morphology in glaucomatous eyes with hemifield defect in a Korean population. *Ophthalmology*. 2019;126:697–701.
30. Burgoyne CF, Quigley HA, Thompson HW, Vitale S, Varma R. Early changes in optic disc compliance and surface position in experimental glaucoma. *Ophthalmology*. 1995;102:1800–1809.
31. Yang H, Reynaud J, Lockwood H, et al. The connective tissue phenotype of glaucomatous cupping in the monkey eye – clinical and research implications. *Prog Retin Eye Res*. 2017;59:1–52.
32. Kadziauskiene A, Jasinskiene E, Asoklis R, et al. Long-term shape, curvature, and depth changes of the lamina cribrosa after trabeculectomy. *Ophthalmology*. 2018;125:1729–1740.
33. Lee SH, Kim TW, Lee EJ, Girard MJA, Mari JM. Lamina cribrosa curvature in healthy Korean eyes. *Sci Rep*. 2019;9:1756.
34. Gage PJ, Rhoades W, Prucka SK, Hjalt T. Fate maps of neural crest and mesoderm in the mammalian eye. *Invest Ophthalmol Vis Sci*. 2005;46:4200–4208.
35. Agoumi Y, Sharpe GP, Hutchison DM, Nicolela MT, Artes PH, Chauhan BC. Laminar and prelaminar tissue displacement during intraocular pressure elevation in glaucoma patients and healthy controls. *Ophthalmology*. 2011;118:52–59.
36. Kotecha A, Russell RA, Sinapis A, Pourjavan S, Sinapis D, Garway-Heath DF. Biomechanical parameters of the cornea measured with the ocular response analyzer in normal eyes. *BMC Ophthalmol*. 2014;14:11.
37. Gordon MO, Beiser JA, Brandt JD, et al. The Ocular Hypertension Treatment Study: baseline factors that predict the onset of primary open-angle glaucoma. *Arch Ophthalmol*. 2002;120:714–720.
38. Medeiros FA, Sample PA, Zangwill LM, Bowd C, Aihara M, Weinreb RN. Corneal thickness as a risk factor for visual field loss in patients with preperimetric glaucomatous optic neuropathy. *Am J Ophthalmol*. 2003;136:805–813.
39. Leske MC, Heijl A, Hyman L, Bengtsson B, Dong L, Yang Z. Predictors of long-term progression in the Early Manifest Glaucoma Trial. *Ophthalmology*. 2007;114:1965–1972.
40. Khawaja AP, Chan MP, Broadway DC, et al. Corneal biomechanical properties and glaucoma-related quantitative traits in the EPIC-Norfolk Eye Study. *Invest Ophthalmol Vis Sci*. 2014;55:117–124.
41. Congdon NG, Broman AT, Bandeen-Roche K, Grover D, Quigley HA. Central corneal thickness and corneal hysteresis associated with glaucoma damage. *Am J Ophthalmol*. 2006;141:868–875.
42. De Moraes CV, Hill V, Tello C, Liebmann JM, Ritch R. Lower corneal hysteresis is associated with more rapid glaucomatous visual field progression. *J Glaucoma*. 2012;21:209–213.
43. Medeiros FA, Meira-Freitas D, Lisboa R, Kuang TM, Zangwill LM, Weinreb RN. Corneal hysteresis as a risk factor for glaucoma progression: a prospective longitudinal study. *Ophthalmology*. 2013;120:1533–1540.
44. Zhang C, Tatham AJ, Abe RY, et al. Corneal hysteresis and progressive retinal nerve fiber layer loss in glaucoma. *Am J Ophthalmol*. 2016;166:29–36.
45. Susanna CN, Diniz-Filho A, Daga FB, et al. A Prospective longitudinal study to investigate corneal hysteresis as a risk factor for predicting development of glaucoma. *Am J Ophthalmol*. 2018;187:148–152.
46. Lee SH, Kim TW, Lee EJ, Girard MJA, Mari JM, Ritch R. Ocular and clinical characteristics associated with the extent of posterior lamina cribrosa curve in normal tension glaucoma. *Sci Rep*. 2018;8:961.
47. Bellezza AJ, Rintalan CJ, Thompson HW, Downs JC, Hart RT, Burgoyne CF. Anterior scleral canal geometry in pressurised (IOP 10) and non-pressurised (IOP 0) normal monkey eyes. *Br J Ophthalmol*. 2003;87:1284–1290.
48. Sigal IA, Flanagan JG, Ethier CR. Factors influencing optic nerve head biomechanics. *Invest Ophthalmol Vis Sci*. 2005;46:4189–4199.

Investigative Ophthalmology & Visual Science